An Improved Analytical Method for Obtaining Cutter Workpiece Engagement In Five-Axis Milling

G. Kiswanto[1], Hendriko[1], E. Duc[2]

[1]Laboratory of Manufacturing Technology and Automation Department of Mechanical Engineering, Universitas Indonesia

[2]Clermont Université, IFMA, UMR 6602, Institut Pascal, BP 10448, F-63000 Clermont-Ferrand, France

Abstract: One of the characteristic of five-axis milling is the tool can be oriented in any direction. And hence the tool orientation could be changed continuously during free-form machining process. It makes the work to predict Cutter Workpiece Engagement (CWE) become more challenging. The existence of tool inclination angle and screw angle will influence the profile of cut geometry. In this paper, an improved method to define lower engagement point (LE-point) is presented. The algorithm was developed by taken into consideration the existence of inclination angle and screw angle. The extended method to calculate *grazing point* in swept envelope development was utilized to define LE-point. The developed model was successfully implemented to generate CWE data with various combination of tool orientation angle. From the test it was found that inclination angle gives significant effect to the location of LE-point. Finally, once CWE data were obtained, feedrate scheduling based on maximum cut area for a given NC code was applied.

Keywords: Five-axis milling, Cutter workpiece engagement, Grazing point

1. Introduction

Nowadays, the ability of the system to generate automatically an optimal process plan is an essential step toward achieving automation, higher productivity and better accuracy [1]. Various studies [1-4] have been conducted to produce a new approach called virtual machining. This new approach is for advancing productivity and quality of machining processes. Manufacturing process include designing, testing and producing the parts is simulated in a virtual environment. This technique tries to decrease the lead-time before the implementation of a new product and to minimize the cycle of the product development. The main purposes of virtual machining in milling operation is how to predict the instantaneous cutting force. They can be used as an input to shorten machining time by optimizing process parameter without sacrificing the machining quality. One of the optimization methods that has become popular in recently is feedrate scheduling [5-7]. Process optimization is performed by adjusting feedrate.

In supporting the machining optimization, the precise geometrical information is very important especially in the modeling and calculating of the cutting force. Various studies [8-10] in geometric simulation strategy based on solid modeling include constructive solid geometry (CSG) and boundary representations (B-Rep) have been conducted. Other researchers used discrete methods such as Z-mapping [11,12], z-buffer [13] and octree method [14,15] for determining engagement region between tool and workpiece along the tool path. Solid modeling gives more accurate information, but computation time significantly increased. Meanwhile discretization methods make the calculation become faster than solid modeling. However, the computation time increases intensely as the precision and accuracy is to be improved.

To overcome such problem, several researchers proposed an analytical method. Ozturk and Lazoglu [16] and Gupta et al. [17] developed analytical method to define the chip load during three axis milling. Tunc and Budak [18] proposed a simple analytical method for five-axis milling that is called bounding point coordinate. Even though the method is fast and accurate,

Corresponding author: E-mail: gandjar_kiswanto@eng.ui.ac.id

ISBN 978 979 8510 61 8

but it is only applicable for flat workpiece surface. Another limitation of the current analytical methods is they cannot provide CWE data with respect to engagement angle. Gupta et al. [17] mentioned that analytical approaches for computing cutter workpiece engagement (CWE) were proven much faster and more accurate compared with the discrete approaches. However study in this method has not been well developed.

Hendriko et al. [19] proposed an hybrid method in defining CWE between flat-end tool and free-form workpiece surfaces. Hybrid model that is a combination of discrete vector model and analytical method was describes in this paper. Workpiece surface is discretized by a number of normal vectors. Then, by using their coordinate and orientation, the surface shape at every instantaneous tool location can be defined mathematically. Another study for obtaining CWE of toroidal cutter during semi finish milling was also proposed by Hendriko et al. [20]. CWE is defined by defining two engagement points, lowermost engagement point (LE-point) and uppermost engagement point (UE-point) as can be seen in

Figure **1**. UE-point (n_f) is calculated by using a method called toroidal boundary method. The proposed model was proven accurate. However, inclination angle and screw angle which are commonly exist in five-axis milling was not taken into consideration. For toroidal cutter, the existence of inclination angle will give significant effect to the coordinate of LE-point (C). The detail about this effect will be discussed in the following section.

This paper presents an improved method to define LE-point that were reported in [20]. The algorithm is developed by considering the existence of inclination angle and screw angle. An extended method to define grazing point in swept volume development is employed for defining the instantaneous lower engagement point (LE-point). At the end of the paper, off-line feedrate scheduling based on cut area prediction is presented for the given NC code.

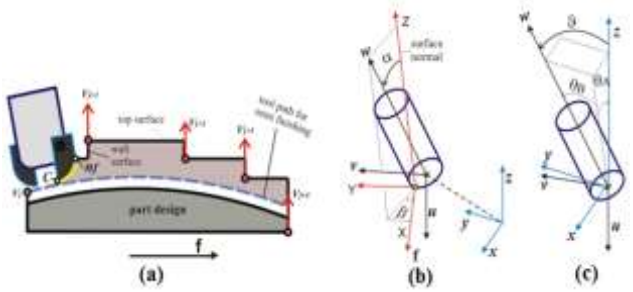

Figure 1. (a) Typical of workpiece surface from rough milling; illustration of the coordinate system, (b) three coordinate frame, (c) tool orientation relative to WCS

2. Establishing Coordinate System and Defining Tool Surface

In five-axis machining, the tool can be rotated in any direction. Part with sculptured surfaces can be machined efficiently by controlling the tool to move and rotate dynamically with respect to the part surface normal (curvatures). For the purpose of analytical representation of moving surface generation of the cutting tool, appropriate operators of the coordinate system transformations are required. Therefore three coordinate systems as illustrated in
Figure **1**b are employed to represent the position and orientation of the tool. They are workpiece coordinate system (WCS) which is the reference coordinate frame, tool coordinate system (TCS), and local coordinate system (LCS). WCS is a fixed framed which is represented by the basis vector *x*, *y*, *z*, while TCS and LCS are denoted by *u*, *v*, *w* and *X*, *Y*, *Z* respectively. The tool inclination angle (□), or in some other references called as lead-angle, and screw angle (□), or also called as tilt angle, are normally used when a sculptured surface part is machined by five-axis milling. They are the angle formed by TCS and LCS as illustrated in
Figure **1**a. The orientation of cutting tool relative to WCS (□) is described as shown in

Figure **1**c, and it is calculated by using the tool orientation relative to *x-axis* (□□) and *y-axis* (□□),

$$\vartheta = \cos^{-1}(\cos\theta_A \cos\theta_B) \tag{1}$$

The operator [M] to map coordinate system from TCS to WCS involving the tool rotation about *x-axis*, *y-axis* and also translation at T is expressed as follow,

$$[M] = \begin{bmatrix} \cos\theta_B & 0 & \sin\theta_B & x_S \\ \sin\theta_A\sin\theta_B & \cos\theta_A & -\sin\theta_A\cos\theta_B & y_S \\ \cos\theta_A\sin\theta_B & \sin\theta_A & \cos\theta_A\cos\theta_B & z_S \\ 0 & 0 & 0 & 1 \end{bmatrix} \tag{2}$$

Where $T(x_T, y_T, z_T)$ is cutter location point (CL-point) which is located at the bottom center of cutting tool. And the tool coordinate frame with orthogonal basis vector *u*, *v* and *w* is defined as,

$$\begin{aligned} w &= [M]\,[0 \quad 0 \quad 1 \quad 0]^T \\ &= [\sin\theta_B \quad -\sin\theta_A\cos\theta_B \quad \cos\theta_A\cos\theta_B]^T \\ v &= \frac{w \times V_T}{|w \times V_T|} \;\; ; \;\; u = v \times w \end{aligned} \tag{3}$$

V_T is the linear velocity from one cutter contact point (CC-point) to the next and it is obtained by,

$$V_T = \frac{C_{C(i+1)} - C_{C(i)}}{f}; \tag{4}$$

Where $C_C(x_{C_C}, y_{C_C}, z_{C_C})$ and f denote the coordinate of CC-point and feedrate, respectively. To calculate the instantaneous CWE, the tool paths will be interpolated linearly. For linear interpolation of the cutting tool movement (translational and rotational), the intermediate position and orientation of cutting tool in between two CC-point is defined as follow,

$$\begin{bmatrix} C_C \\ \theta_A \\ \theta_B \end{bmatrix} = \begin{bmatrix} C_{C(i)} \\ \theta_{A(i)} \\ \theta_{B(i)} \end{bmatrix} + p \begin{bmatrix} C_{C(i+1)} - C_{C(i)} \\ \theta_{A(i+1)} - \theta_{A(i)} \\ \theta_{B(i-1)} - \theta_{B(i)} \end{bmatrix} \tag{5}$$

where p denote the tool path interpolation parameter.
In this study, the CWE model is developed for toroidal cutter. The typical of its surface is decomposed into toroidal (S_T) and cylindrical (S_C) parametric surfaces as shown in Figure 2. The representations of toroidal surface and cylindrical surface with respect to the tool coordinate system (TCS) is described as,

$$\begin{aligned} &S_T(\varphi;\lambda) \\ &= [(r_m + r\sin\lambda)\sin\varphi \quad (r_m + r\sin\lambda)\,\mathrm{cc} \end{aligned} \tag{6}$$

$$S_C(\varphi; l_k) = [R\sin\varphi \quad R\cos\varphi \quad l]^T \tag{7}$$

Where r is minor radius of cutting tool, r_m is the distance between cutter centre point to minor radius, R is major radius of cutter, and l is height of cutter measured from the bottom. While λ and φ denote the toroidal angle and the engagement angle, respectively. Due to the cutter location (Cl) data and workpiece surface information are provided in workpiece coordinate system (WCS), then the cutter surface is mapped from TCS to WCS.

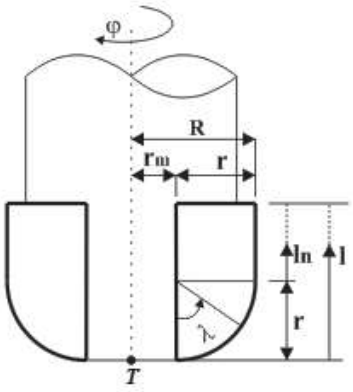

Figure 2. Geometry of toroidal cutting tool

$$S_C{}'(x'_{S_C},\ y'_{S_C}, z'_{S_C}) = [\mathrm{M}]\ S_C(\varphi; \mathrm{l_k}) \quad (8)$$

$$S_T{}'\left(x'_{S_T},\ y'_{S_T}, z'_{S_T}\right) = [\mathrm{M}]\ S_T\ (\varphi; \lambda) \quad (9)$$

3. Obtaining Upper Engagement Point

As mentioned in Introduction that CWE is determined by defining two engagement points, UE-point (n_f) and LE-point (C). In this paper the method to define UE-point will not be discussed deeply. The detail mechanism was presented in [20]. The same mechanism will be used for the application purpose.

Because of toroidal cutter has two surfaces, cylindrical surface and toroidal surface, then the method to define UE-point when located on cylindrical surface is different from that on toroidal surface. When UE-point located on the cylindrical surface, the coordinate of UE-point can be calculated by using Eq.(**Error! Reference source not found.**) after the length of cut (l_n) is obtained. A method called *Cylindrical-boundary* is used to define the length of cut. l_n can be determined if at least one of the axis component of UE-point, $n_f(x_{nf}, y_{nf}, z_{nf})$, is known. For example, when the UE-point is located on the wall of workpiece block as shown in Figure 3a, then x_{nf} is equal to x_B. In this case, l_n is calculated by using *X-Cylindrical method*, on the other hand, *Z-Cylindrical method* is used when it is located on the top of workpiece surface (Figure 3b).

Meanwhile when UE-point is on toroidal side, then its coordinate can be determined by using Eq.(**Error! Reference source not found.**) after its toroidal angle (λ_n) is obtained. It is calculated by using a method called *Toroidal-Boundary Method*. This method consists of *X-toroidal* when UE-point is located on the wall surface (Figure 3c), and *Z-toroidal method* when it is located on the top surface (Figure 3d).

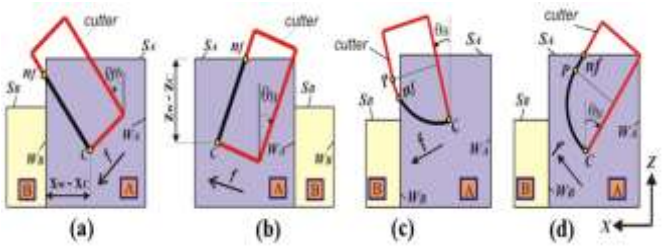

Figure 3. Two possible location of UE-point for cylindrical side
(a) wall of workpiece, (b) top of workpiece; and toroidal side
(c) wall of workpiece, (d) top of workpiece

4. Obtaining Lower Engagement Point

According to Gani et al. [21], tool inclination in five axis milling has a large influence on the cut geometry. It will not only change the chip thickness, but also the length of cut. In term of cutting force, previous studies [8-10] showed that negative inclination angle tend to give higher cutting force. It is believed due to the larger contact area between cutter and workpiece.

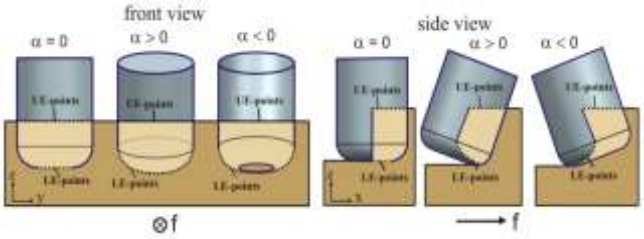

Figure 4 Effect of inclination angle to LE-point

LE-point of toroidal cutter with respect to inclination angle and as a function of engagement angle are illustrated in Figure 4. It can be seen that when machining without inclination angle, LE-points at every engagement angle are located at the bottom of front cutting edge or at toroidal angle of LE-points (λ_C) equal to zero. However, when inclination angle exist, then the coordinate of LE-points change significantly. When $\alpha > 0$, LE-points is located at the front cutting edge with $\lambda_C > 0$. Meanwhile, if $\alpha < 0$, LE-points is at the back cutting edge with $\lambda_C > 0$.

The method to define toroidal angle of LE-point will be derived from the method to define swept envelope. As mentioned by [22-24] that the swept envelope is constructed by three points, forward boundary (egress point), envelope boundary (grazing point) and backward boundary (ingress point). Grazing point is considered as LE-point at every engagement angle. It is obtained by using the tangency function $F_{(\vartheta,\varphi,p)} = N_{S_T(\vartheta,\varphi,p)}.V_{S_T(\vartheta,\varphi,p)} = 0$, which consists of the cutter surface normal $N_{S_T(\vartheta,\varphi,p)}$ and the cutter moving vector $V_{S_T(\vartheta,\varphi,p)}$. With the same method, LE-points at every engagement angle is calculated. Even though toroidal cutter is constructed by two sides, LE-point is only located on toroidal side.

The surface normal of an arbitrary point Q on toroidal surface in TCS is described by,

$$N_{S_T} = \frac{\partial S_T/\partial\lambda}{|\partial S_T/\partial\lambda|} \times \frac{\partial S_T/\partial\varphi}{|\partial S_T/\partial\varphi|} = [\sin\lambda.\sin\varphi \quad \sin\lambda.\cos\varphi \quad -\cos\lambda] \tag{10}$$

When Eq.(**Error! Reference source not found.**) is transformed to the moving frame, it yields to,

$$N_{S_T'(\vartheta,\varphi,p)} = \sin\lambda.sin(\varphi).\boldsymbol{u} + \sin\lambda.\cos(\varphi).\boldsymbol{v} - \cos\lambda.\boldsymbol{w} \tag{11}$$

The velocity of an arbitrary point Q on the toroidal surface (V_{S_T}) is determined as follow,

$$V_{S_T} = V_T + \omega \times \overrightarrow{TQ} \tag{12}$$

where ω and $\overrightarrow{TQ}$ denote the angular velocity and the position vector from T to Q, respectively. Because of the tool orientation change for any instantaneous position has been adjusted in Eq.(**Error! Reference source not found.**), then it is assumed that $\omega = 0$. And hence the velocity vector in Eq.(**Error! Reference source not found.**) is equal to V_T and the tangency function yield to,

$$\begin{aligned} F_{(\vartheta,\varphi,p)} = & \sin\lambda_C \,.\, sin(\varphi) \,.\, (V_T.\boldsymbol{u}) \\ & + \sin\lambda_C \,.\, \cos(\varphi) \,.\, (V_T.\boldsymbol{v}) \\ & + \cos\lambda_C \,.\, (V_T.\boldsymbol{w}) = 0 \end{aligned} \tag{13}$$

Finally, toroidal angle of the LE-point as a function of engagement angle ($\lambda_{C(\varphi)}$) is calculated as follow,

$$\lambda_{C(\varphi)} = \tan^{-1}\left[\frac{V_T.\boldsymbol{w}}{\sin(\varphi).(V_T.\boldsymbol{u}) + \cos(\varphi)\,.\,(V_T.\boldsymbol{v})}\right] \tag{14}$$

By applying $\lambda_{C(\varphi_C)}$ into Eq.(**Error! Reference source not found.**), then coordinate of LE-point is obtained.

$$C\,(x_C, y_C, z_C) = [\mathrm{M}]\, S_T\,(\varphi; \lambda_C) \tag{15}$$

5. Cut Geometry Calculation

Since λ_{n_f}, λ_C and l_n were obtained, then the geometry of cut can be calculated. In toroidal cutter, l_n is the length of engagement on cylindrical side. And hence it is equal to zero when n_f located on toroidal side. On the other hand, $\lambda_n = 90$ when CWE is on cylinder side. The length of cut (q) is determined by this equation,

$$q = \frac{\pi.r}{180}(\lambda_n - \lambda_C) + l_n\,; \quad (\pi = 3.14) \tag{16}$$

The machining optimization will be performed based on the generated cut area at instantaneous tool location. Before cut area will be calculated, cut thickness should be determined. According to Kumanchik and Schmitz [25], the cut thickness in milling is defined as the distance between the current tooth path and the previous tooth path along the line segment connecting the tool center to the current tooth cutting edge. However, this definition is only applicable for machining with perpendicular tool orientation. Inclination angle should be taken into consideration as another factor that influences the size of cut thickness. Tool inclination makes the cut thickness smaller than the distance of two consecutive tooth paths. Therefore, cut thickness (h) as a function of engagement angle is expressed as,

$$h = f\ \cos\alpha\ \sin\varphi \tag{17}$$

Finally, the cross cut area (A_φ) is calculated by multiplying the cut thickness by cut width.

$$A_{\varphi} = q.h \tag{18}$$

6. Implementation and Discussion

Based on the formulae derived in the previous sections, a simulation program using MATLAB has been developed, enabling the calculation of CWE and also the cross cut geometry. One part design and workpiece surface as shown in Figure 5a was tested. Machining conditions used in the test were feedrate 0.2 mm/rot and spindle speed 4000 rpm. Two teeth toroidal cutter with diameter 25 mm and minor radius 6 mm was employed as cutting tool.

By using the developed simulation, the shape and the size of cut can be generated. The shapes of cut generated by the program simulation are shown in Figure 5b. In this figure, the tool was set with $\alpha = 0$ and $\beta = 0$. It can be seen that the shape of cut at the top side resembles the shape of workpiece surface and that one at the bottom side resembles the shape of part surface. It is an indication that the

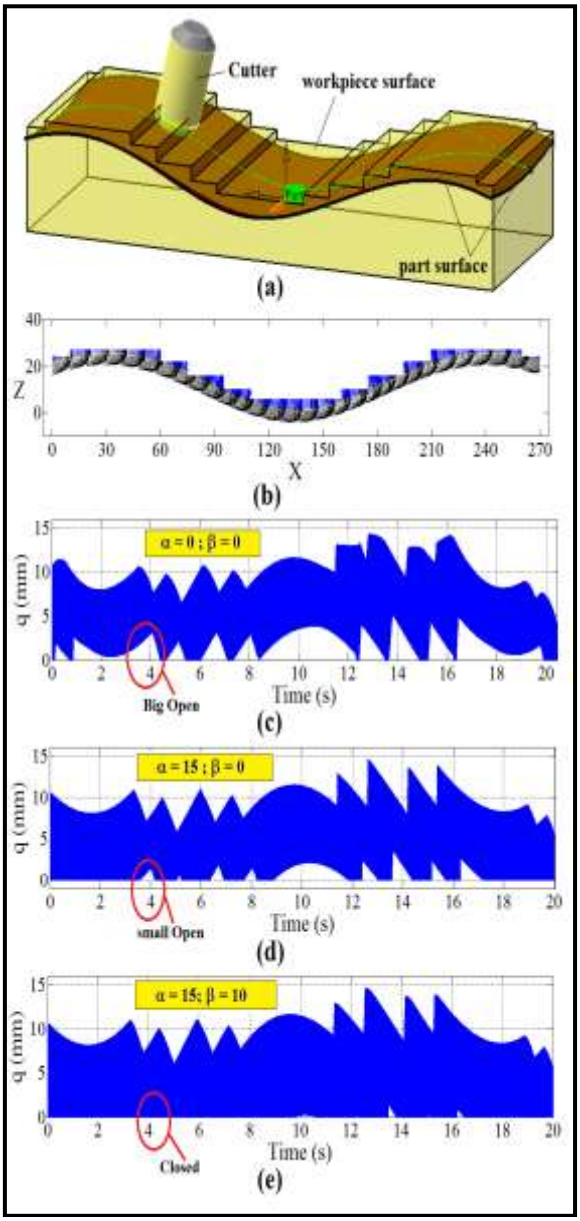

Figure 5. (a)Test model; (b) CWE progression; length of cut from (c) Test 1 ($\alpha = 0;\ \beta = 0$), (d) Test 2 ($\alpha = 15;\ \beta = 0$), (e) Test 3 ($\alpha = 15;\ \beta = 10$)

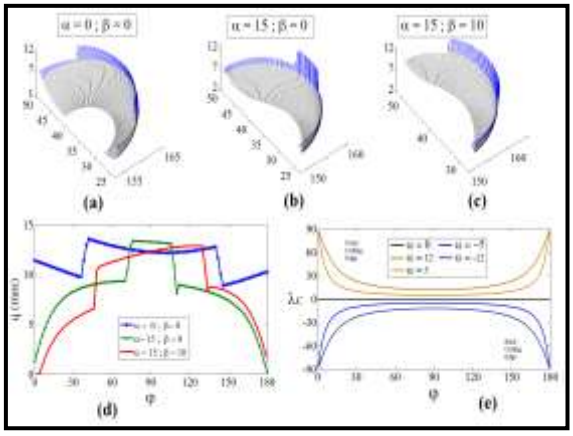

Figure 6. Geometry of cut (a) Test 1, (b) Test 2, (c) Test 3, and (d) the length of cut for CC-37, (e) Effect of inclination angle on toroidal angle of LE-point

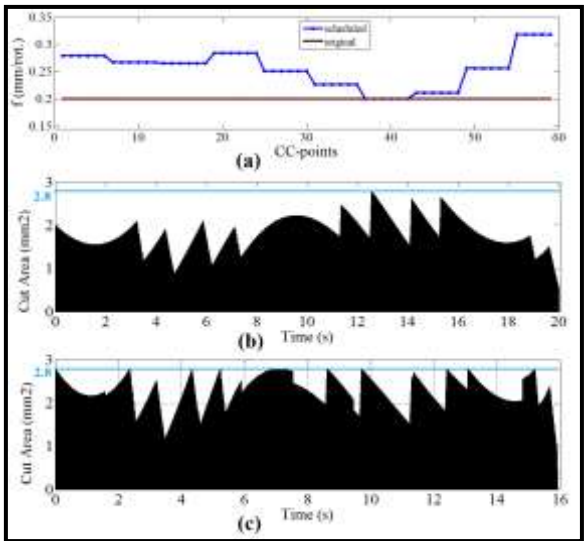

Figure 7. Machining optimization for Test 2, (a) feedrate scheduling; cut area and machining time from (b) original feedrate,(c) scheduled feedrate

proposed method is accurate. Cut width or the length of cut in one tool pass for various tool orientations are presented in Figure 5c ($\alpha = 0$; $\beta = 0$/Test 1), Figure 5d ($\alpha = 15$; $\beta = 0$/Test 2), and Figure 5e ($\alpha = 15$; $\beta = 15$/Test 3). In these graphs, the CWE data were generated for every $8x10^{-5}$ second of tool motion. It can be seen that every graph shows different profile especially at the bottom side. As highlighted by red circle at the bottom, Test 1 shows 'big open' profile, meanwhile Test 2 depicts 'small open' profile and Test 3 shows 'closed' profile. 'Open' profile appears when CWE occurred in one tool rotation, meanwhile 'Closed' profile appear when there are some part of cutting tool in one tool rotation do not contact with workpiece. This condition can be explained clearly by referring to Figure 6.

Figure 6 displays the shape and length of cut as a function of engagement angle for CC point 37. In this figure, the shape of cut from various combination of tool orientation are presented. The cut with straight and blue line on the top is an indication that the UE-point is located on the cylindrical side. In this case, the engagement is occurred on both cylindrical and toroidal side. If there is no such line on the top, it means that the engagement is only occurred on the toroidal side. Figure 6a show the shape of cut for Test 1. It can be seen that the shape of cut at the bottom side resemble the shape of bottom side of cutting tool. Different phenomena are showed by Figure 6b (Test 2) and Figure 6c (Test 3). When the tool inclination angle exist then the location of LE-point become very dynamic. And hence, the shape of cut at the bottom

ISBN 978 979 8510 61 8

side do not resemble the bottom side of cutting tool. Figure 6d present the length of cut for all tests. It can be seen that Test 1 produces large CWE in one tool rotation ($\varphi \in \{0,180\}$). This condition will produce 'big open' profile as highlighted in Figure 5c. Test 2 generates more dynamic length of cut and small engagement occurred in beginning. Small CWE in beginning creates 'small open' profile as highlighted in Figure 5d. On the other hand, Test 3 also shows dynamic length of cut, but there is no engagement in beginning. This is the answer why 'closed' profile appear in Figure 5d .

One test for checking the effect of inclination angle to the location of LE-point was also performed. The location of LE-point as depicted in Figure 6e is represented by its toroidal angle. When the tool without inclination angel, then LE-point at every engagement angle will be located at the bottom of front cutting edge ($\lambda_C = 0$). However, when positive inclination angle exist, LE-point will be located at front cutting edge with $\lambda_C > 0$. It can be seen that increasing inclination angle will increase λ_C. For positive inclination angle, bigger λ_C produces smaller length of cut. Similar to positive inclination angle, increasing negative inclination angle will also increase λ_C. The sign minus (-) for λ_C is only to indicate that LE-point is located at the back cutting edge. However, increasing λ_C tends to produce larger length of cut, this is due to the engagement occurred not only at front cutting edge but also possible at the back cutting edge.

Once the geometry of cut is obtained, then machining optimization can be performed. Feedrate scheduling strategy based on the maximum cut area was performed for Test 2 ($\alpha = 15$ and $\beta = 0$) as shown in Figure 7a. To avoid instability due to the continuous feedrate change, then the tool path is divided into NC block which contain 6 consecutive CC-points. Optimization was performed based on the largest cut area generated in every NC block. As can be seen in Figure 7b, the cross cut area at CC-point 37 with $cut\ area = 2.8\,mm^2$ is found to be the largest. Thus, it was selected as the reference. The feedrate at others CC-points were optimized by comparing their cut area with the reference. The results show that the feedrate increase when cut area decrease, and vice versa. Hence, most cut area generated from optimization was found larger than original feedrate and with smaller variation. The machining time before and after feedrate scheduling can be compared from Figure 7b and Figure 7c. It can be seen that the total machining time was successfully reduced from 20.4 second with original feedrate to become 15.87 second with feedrate scheduling. It shortens the time about 22.2%. However in other cases, the controlled/scheduled feedrate may produce longer machining time since the original feedrate might be too high.

7. Conclusion

An improved method to predict Cutter Workpiece Engagement during semi finish milling has been developed. The method involves the calculation of LE-point when the inclination angle and screw angle exist. The formulation derived has been implemented in a computer simulation. By using the simulation program, the geometry and length of cut at instantaneous tool position can be generated. From the test it was found that inclination angle gives significant effect to the location of LE-point. Finally, once CWE data were obtained, feedrate scheduling based on maximum cut area for a given NC code was applied. From this optimization, the machining time was successfully reduced.

8. References

[1] El-Mounayri H, Spence AD, Elbestawi MA. Milling Process Simulation-A generic Solid Modeller Based Paradigm, Journal of Manufacturing Science and Engineering 1998; 120(2):213-221.

[2] Yun W.S, Chow DW, Ehmann KF. Development of a virtual machining system, part 1: approximation of the size effect for cutting force prediction, International Journal of Machine Tools & Manufacture 2002; 42(15):1595-1605.

ISBN 978 979 8510 61 8

[3] Yun W.S, Ko JH, Chow DW. Development of a virtual machining system, part 2: prediction and analysis of a machined surface error, International Journal of Machine Tools & Manufacture 2002; 42(15):1607-1615.
[4] Merdol SD, Altintas Y. Virtual Cutting and Optimization of three axis milling processes, International Journal of Machine Tool & Manufacture 2008; 48 (10):1063-1071.
[5] Dong J, Ferreira PM, Stori JA. Feed-rate optimization with jerk constraints for generating minimum-time trajectories. International Journal of Machine Tools & Manufacture 2007; 47(12-13): 1943-1955.
[6] Baek DK, Ko TJ. Feedrate scheduling for free-form surface using an NC verification model. International Journal of Machine Tool & Manufacture 2008; 48(2):163-172.
[7] Erdim H, Lazoglu I. Feedrate scheduling strategies for free-form surfaces. International Journal of Machine Tool & Manufacture 2006; 46(7-8): 747-757.
[8] Altintas Y, Spence AD. End milling force algorithms for CAD systems. Manufacturing Technology CIRP Annuals 1991; 40:31-34.
[9] Spence AD, Altintas Y. A solid modeler based milling process simulation and planning system. Trans ASME J. Eng. Ind. 1994;116:61–69.
[10] El-Mounayri H, Spence AD, Elbestawi MA. Milling process simulation: a generic solid modeller based paradigm. J. Manuf. Sci. and Eng. 1998; 120:213-221.
[11] Lazoglu I. Sculptural surface machining: a generalized model of ball-end milling force system. Int. J. Mach. Tools and Manuf. 2003; 43:453–462.
[12] Kim GM, Chu CN. Mean cutting force prediction in ball-end milling using force map method. Journal of Materials Processing Technology 2004; 146:303–310.
[13] Fussel BK, Jerrard RB, Hemmet JG. Modeling of cutting geometry and forces for 5-axis sculptured surface machining. Computer Aided Design 2003; 35:333-346.
[14] Li GJ, Yao YX, Xia PJ, Liu CQ, Wu C Extended octree for cutting force prediction. Int. J. Mach. Tools and Manuf. 2008; 39:866-873.
[15] Kim YH, Ko SL. Improving of cutting simulation using the octree method. Int. J. Adv. Manuf. Technol. 2006; 28:1152-1160.
[16] Ozturk B, Budak E. Modeling of 5 axis milling processes. Min .Sci. Technology 2006; 11 : 287-311.
[17] Gupta SK, Saini SK, Spranklin BW, Yao Z. Geometric algorithms for computing cutter engagement functions in 2.5D milling operations. Computer Aided Design 2005; 37: 1469-1480.
[18] Tunc LT, Budak E. Extraction of 5 axis milling conditions from CAM data for process simulation. Int. J. Adv. Manuf. Technol. 2009; 43:538-550.
[19] Hendriko, Duc E, Kiswanto G. Analytical method for obtaining Cutter Workpiece Engagement in Five-Axis Milling. Part 3: Flat-end Cutter and Free-Form Workpiece Surface. Proceeding of 23rd International Conference of Flexible Automation and Intelligent Manufacturing, 2013, Porto, Portugal.
[20] Hendriko, Duc E, Kiswanto G. Analytical cut geometry prediction for free form surface during semi-finish milling, Proceding of the 8th ASME Manufacturing Science and Engineering Conference, 2013, Madison, Wisconsin, USA.
[21] Gani EA, Kruth JP, Vanherck P, Lauwers B. A geometrical model of the cut in five axis milling for the influence of tool orientation. Int. J. Adv. Manuf. Technol. 1997; 13: 677-684.
[22] Chiou CJ, Le YS. Swept surface determination for five-axis numerical control machining, Int. J. Mach. Tools and Manuf. 2002; 42 : 1497-1507.
[23] Weinert K, Du S, Damm P, Stautner M. Swept volume generation for the simulation of machining processes, Int. J. Mach. Tools and Manuf. 2004; 44 : 617-628.
[24] Du S, Surmann T, Webber O, Weinert K. Formulating swept profile for five-axis tool motions, Int. J. Mach. Tools and Manuf. 2005; 45 : 849-861.
[25] Kumanchik LM, Schmitz TL. Improved analytical chip thickness model for milling. Precision Engineering 2007; 31:317-324.

ISBN 978 979 8510 61 8